A Novel Model for Measuring the Amount of Four Pesticides with Rapid Safety Classification

Natthasak Yaemsuk and **Suchart Yammen**[†], Non-members

ABSTRACT

According to the Food and Agriculture Organization of the United Nations (FAO) reports that approximately 4.5 million tons of pesticides are used worldwide per year, and estimates that pesticide poisoning causes approximately up to 40,000 deaths per year. This research proposes a novel exponential with constant parametric model for evaluating the levels of pesticide residues on vegetables. The original contribution lies in the model's capability to predict the maximum spectral power density (MSPD) in [μW/cm²] from reflected light spectrum signals when integrated with our previously portable developed VIS-NIR spectrometer. To evaluate the performance of the proposed model, experiments were conducted via four test pesticides carbendazim, cypermethrin, diazinon, and imidacloprid across ten different concentration levels ranging from one to ten milligrams per liter. The results demonstrate superior performance with the highest R^2 score and the lowest root mean squared error (RMSE), and precisely achieve the safety levels of the four pesticide residues according to maximum residue limits (MRL) with the Accuracy of one and the harmonic mean recall specificity (HMRS) of one when compared to the line equation, quadratic and partial least squares regression (PLSR) models.

Keywords: exponential plus constant model, line equation model classification, maximum spectral power density (MSPD)

1. INTRODUCTION

The Food and Agriculture Organization (FAO) reports global pesticide usage of approximately 4.5 million tons annually [1], estimated pesticide poisoning causing 20,000–40,000 deaths per year [2]. These chemicals persist in environmental systems for extended periods, and despite bans in developed nations, their usage continues in many developing countries [3]. Consequently, there is an urgent need for rapid, accurate on-site pesticide residue detection methods. This necessity has driven the development of portable detection devices based on visible and near-infrared (VIS-NIR) spectroscopy, a technique that is cost-effective, environmentally sustainable, requires minimal sample preparation, and is suitable for both qualitative and quantitative analysis [4-12]. Tsagkaris et al. [13] reviewed light-based detection methods for pesticide residues, demonstrating their potential for efficient food monitoring. Similarly, Zainurin et al. [14] developed an ESP32-based portable spectrometer for measuring various contaminants in water, while Nazarloo et al. [15] applied VIS/NIR spectroscopy for non-destructive detection of profenofos residues in tomatoes.

The development of field-deployable spectrometers, however, faces significant challenges. A primary obstacle is the nonlinear relationship of spectral data and pesticide concentrations, which is compounded by environmental interferences (temperature, humidity, pressure) that introduce variability. Therefore, enhancing data quality by applying smoothing techniques and multivariate scatter correction (MSC), in addition to developing predictive models using various methods such as partial least squares discriminant analysis (PLS-DA), PLSR, and advanced approaches like one-dimensional convolutional neural networks (1D-CNN) and deep transfer learning (DTL), remains critical. Heydarov et al. [16] designed a portable spectrometer employing support vector machines (SVM) and convolutional neural networks (CNN) for food spectral analysis, while Nazarloo et al. [17] combined VIS/NIRS with PLSR and artificial neural networks (ANN) for pesticide residue detection in tomatoes. Additionally, Li et al. [18] utilized spectral data across 216 bands (950 nm −1,666 nm) with pre-processing methods and the corrective adaptive reweighted sampling (CARS) algorithm to detect toxins in cabbage flowers, achieving an R^2 of 0.9688. Rodriguez et al. [19] employed NIR spectroscopy with PLS to predict chlorpyrifos-methyl levels in rice varieties, and Sun et al. [20] integrated spectral analysis with CNN, developing a model with an R^2 of 0.883. Further studies using comparable approaches are documented in [21–25].

The computational complexity of the previous methods presents a significant constraint for portable spectrometers operating on microcontrollers (MCUs). Nevertheless, NIR spectral data typically exhibit characteristic peaks corresponding to chemical bond vibrations within samples. Aira et al. [26] demonstrated a curve-fitting plot for diffuse reflectance at five-hundred-sixty-nanometres wavelength for each glyphosate concentration obtained from a linear polynomial model with

Manuscript received on March 31, 2025; revised on May 15, 2025; accepted on May 23, 2025. This paper was recommended by Associate Editor Siraporn Sakphrom.

The authors are with Department of Electrical and Computer Engineering, Faculty of Engineering, Naresuan University, Phitsanulok, 65000, Thailand.

[†]Corresponding author: sucharty@nu.ac.th

Digital Object Identifier: 10.37936/ecti-eec.2525232.258569

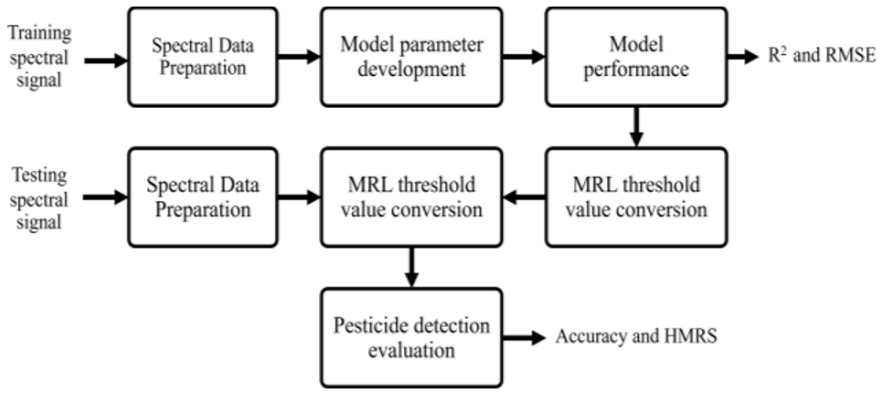

***Fig. 1**: An overview of the research methodology.*

a R-square score of 0.9106, and facilitated pesticide concentration prediction and detection without excessive computational requirements.

However, linear models often provide insufficient accuracy for this application. Various calibration curve models have been developed to enhance prediction precision. Dinesha et al. [27] applied spectrophotometric methods to construct a standard curve for Coragen concentration prediction, achieving an R^2 of 0.976. Zohar et al. [28] and Zhang et al. [29] determined that higher-order polynomial models are sometimes necessary to capture nonlinear relationships. ABASS et al. [30] implemented a quadratic polynomial model to address these nonlinearities, and Ostertagová [31] and Elshewey et al. [32] demonstrated the superiority of this approach over linear models. Zahedi et al. [33] and Locascio et al. [34] also developed polynomial models offering enhanced flexibility in capturing complex spectral behaviour while Zhang et al. [35], Wang et al.'s [95] and Hu et al. [96] proposed that exponential regression models may be optimal for pesticide residue concentration prediction compared to linear and quadratic approaches.

Based on these considerations in recent research, Natthasak and Suchart [36] successfully detected four pesticides namely Carbendazim, Cypermethrin, Diazinon, and Imidacloprid on chili samples by identifying MSPD at specific wavelengths on the developed residue profiles of each of the four pesticides. Unfortunately, there has been no study on concentration prediction in terms of its ability to estimate pesticide concentrations and to be used as a safer warning for consumption of vegetables and fruits. Therefore, a proposed parametric model is presented, which provides the desired concentration prediction values for the four target pesticides on chili. The performance evaluation of the proposed model is compared with first- and second-order polynomial models.

This paper is divided into four sections: Introduction, Methods, Results, and Conclusions. Section II details the spectral data collection, parametric model development, and model performance with evaluation metrics. Next, Section III presents the experimental results and discussions, and Section IV summarizes the main findings and proposes directions for future research.

2. MATERIALS AND METHOD

This section describes the methodology for collecting spectral data and developing both the proposed model and the comparative models using the MSPD from the training dataset. It also covers the MRL standard in mg/L and its conversion to spectral power density (SPD) in the unit of [μW/cm^2]. Additionally, it explains the MSPD classification process for determining "Safe" status or "Unsafe" status, along with the evaluation of model performance.

2.1 Spectral Data Collection

Previous research by Natthasak and Suchart [36] had already demonstrated the high efficiency of a VIS-NIR portable spectrometer that can measure spectral values in [μW/cm^2] at eighteen different wavelengths: 410 nm, 435 nm, 460 nm, 485 nm, 510 nm, 535 nm, 560 nm, 585 nm, 610 nm, 645 nm, 680 nm, 705 nm, 730 nm, 760 nm, 810 nm, 860 nm, 900 nm, and 940 nm. As we known that properties of the four pesticides give spectral peaks at different wavelengths. For example, the spectral peak values for carbendazim, cypermethrin, diazinon, and imidacloprid occur at wavelengths of 460 nm, 535 nm, 900 nm, and 810 nm, respectively.

In the preparation procedure, 480 chili samples with pesticide residues obtained from a field in Phitsanulok, Thailand, were carefully processed within the laboratory environment complying with ISO/IEC 17025:2005 and ISO/IEC 17025:2017 [37, 38].

The model development required input data in the form of MSPD values, which were derived from diffuse reflectance spectra. These spectra were obtained when the portable VIS-NIR spectrometer developed by Natthasak and Suchart [36] was applied to four pesticide residues on chili seeds samples at ten different concentrations: 1, 2, 3, 4, 5, 6, 7, 8, 9, and 10 [mg/L].

The simplest class of either line equation or polynomial modeling problems is concerned with phenomenon that are describable by the MSPD value and a specific

pesticide concentration as designated by the symbols $x_i[n]$ and $n, i \in 1, 2, 3, 4$ represents a type of the four pesticides on chili samples; that is, Carbendazim ($i = 1$), Cypermethrin ($i = 2$), Diazinon ($i = 3$) and Imidacloprid ($i = 4$).

To ensure the developed model's stability in accurately and precisely approximating the MSPD for the pesticides, the researchers divided the data into a training set of 320 samples for determining the model's parameters and a test set of 160 samples for evaluating the model's efficiency. The 2:1 ratio of training to testing samples is suitable for evaluating the model's performance, as the test set will serve as new data to assess the accuracy and precision of the approximation process using the parameters obtained from the training set.

For the purpose of this presentation, it is useful to interpret the independent value $x_i[n]$ as the cause value and n as the associated effect value. If the data points tend to lie on a straight line, a commonly used model for relating the $y_i[n]$ and n of this data set would be a line equation model [39 - 47] which takes the form:

$$y_i[n] = a_1 n + a_0 \tag{1}$$

The objective of the line equation modeling is clearly assigned values to the slope parameter a_1 and the vertical axis intercept parameter a_0 so that this line equation model best fits the given data points in some well-defined sense. On the other hand, a more appropriate model might be a quadratic model [48 - 55] in which each of the $y_i[n]$ values with respective to the index n representing as a non-negative real number n. The estimated data element is given by

$$y_i[n] = a_2 n^2 + a_1 n + a_0 \tag{2}$$

As with the line equation model sense, the parameters a_0, a_1, and a_2 of quadratic model are selected so that this hypothesized model best fits given data points in some well-defined sense. The optimum line equation or quadratic fit in the least squares error sense is also discussed in [56 - 63].

In addition, nine sets of SPD data per pesticide concentration level were used as training data for the PLSR method [87], which combines the concepts of principal component analysis (PCA) [88, 89] with polynomial regression to obtain MSPD estimates at each concentration level. These estimates are denoted by the sequence symbols $x_i^P[n]$, where $n \in 1, 2, 3, ..., 10$ represents the concentration levels as non-negative integers. The MSPDs for $y_i[n]$ ranging from 0 to 11 mg/L as shown in Table 2.

The next section presents a novel approach to develop the optimal parameters for the proposed exponential-plus-constant model.

2.2 Exponential Model Development

In general data analysis, the synthesis of line equation or polynomial models has so far been directed toward the tracking trend that are either line or polynomial in nature. The concept of our proposed model is now generalized to the case where the trend of the spectral sequence being tracked is equal to a linear combination of exponentials, given by:

$$y_i[n] = a_0 e^n + a_1 a_2^n \tag{3}$$

where $y_i[n]$ is the estimated values of the spectral data sequence at a specific pesticide concentration (n) ranging from 1 mg/L to 10 mg/L for $n \in 1, 2, 3 \ldots, 10$.

To predict the present behaviour of the given spectra sequence $\{x_i[n]\}$ based on knowledge of the past spectra element values is clearly a valuable asset to know the concentration of toxic residues in vegetables and fruits at a level that can be safely consumed. The linear combination of exponentials in relationship (3) is instructive when consider the simplest case of the given spectra sequence whose values satisfy the homogeneous linear non-recursive relationship given by

$$x_i[n] - \alpha x_i[n-1] - \beta x_i[n-2] = 0 \tag{4}$$

for all integers n where the two fixed scalars α and β can be either real or complex number. Given that the second term in Eq. (3) holds for all integer values of concentration n, This study inserts it into the underlying homogeneous linear non-recursive relationship in Eq. (4) to establish the relationship between the two scalarsα and β, that is,

$$\alpha = e - \beta e^{(-1)} \tag{5}$$

Substituting the real scalar α in Equation (5) into the linear relationship in Equation (4) yields:

$$x_i[n] = e x_i[n-1] - \beta(e^{(-1)} x_i[n-1] - x_i[n-2] \tag{6}$$

To determine the optimum scalar β that tracks the spectral sequence $\{x_i[n]\}$, the fidelity of approximation is measured by the sum of squared error magnitudes; that is,

$$f(\beta) = \sum_{n=3}^{10} \left| x_i[n] - e x_i[n-1] + \beta(e^{-1} x_i[n-1] - x_i[n-2]) \right|^2 \tag{7}$$

A necessary condition for this sum of squared errors to be minimized is that the derivative of f(β) with respect to the real variable β zero. This leads to the optimum value of the scalar β^0, specified by:

$$\beta^0 = \frac{\sum_{n=3}^{10} (x_i[n] - e x_i[n-1])(x_i[n-2] - e^{-1} x_i[n-1])}{\sum_{n=3}^{10} (e^{-1} x_i[n-1] - x_i[n-2])^2} \tag{8}$$

Substituting the above optimum scalar β^0 into Equation Eq. (5), the optimum scalar α^0 is given by

$$\alpha^0 = e - \beta^0 e^{-1} \tag{9}$$

Both optimum scalars α^0 and β^0 appear in the linear relationship of Equation (4), and the optimum coefficient

a_2^0 obtained from the associated polynomial equation is given by

$$\alpha_2^0 = -\beta^0 e^{-1} \tag{10}$$

Then, the optimum coefficient a_2^0in Eq. (10) substituted into the relationship in Eq. (3) results in

$$y_i[n] = a_0(e)^n + a_1(-\beta^0 e^{-1}) \tag{11}$$

The determination of the two optimum coefficients a_1 and a_0 for tracking the spectral sequence $\{x_i[n]\}$ is then sought. Again, the fidelity of approximation is measured by the sum of squared error magnitudes, specified by:

$$g(a_0, a_1) = \sum_{n=1}^{10} \left| x_i[n] + a_0(e)^n - a_1(a_2^0)^n \right|^2 \tag{12}$$

The exponential model parameters in Eq. (11) are to be selected so that the error function $g(a_0, a_1)$ as specified by Eq. (12) is minimized in the sum of model error sense. Therefore, the optimum coefficients a_0^0 and a_1^0 can be obtained by the normal equation [64 – 68, 70, 71]

$$(Z^T Z)\bar{a} = Z^T \bar{x} \tag{13}$$

where $\bar{x}$ is a 10×1 vector with elements $x_i[n]$ for $n \in 1, 2, 3\ldots, 10$, $\bar{a} = [a_0^0 \ a_1^0]^T$ is an 2×1 optimum vector, and Z is a 10×2 matrix with elements given by

$$Z = \begin{bmatrix} e^1 & (a_2^0)^1 \\ e^2 & (a_2^0)^2 \\ e^3 & (a_2^0)^3 \\ \vdots & \vdots \\ e^9 & (a_2^0)^9 \\ e^{10} & (a_2^0)^{10} \end{bmatrix} \tag{14}$$

Moreover, since the two parameter roots: a_2^0 and e are nonzero and distinct, it follows that the data matrix $Z^T Z$ is invertible [69, 72 - 80]. Therefore, the optimum parameters a_1^0 and a_0^0 are obtained by the left multiplying each side of the normal relationship in Eq. (13) by the inverse matrix $(Z^T Z)^{-1}$ to give

$$\bar{a} = (Z^T Z)^{-1} Z^T \bar{x} \tag{15}$$

After obtaining the parameters according to Eq. (10) and Eq. (13) for the developed exponential model in Equation (11), the model was trained using the MSPD data of four pesticides carbendazim, cypermethrin, diazinon, and imidacloprid within the concentration range of 1 mg/L to 10 mg/L, as described in Section 2.2. This exponential model was then applied to approximate the MSPD values of each pesticide as a function of its concentration. The objective was to determine the threshold values of reflectivity power density that correspond to the MRL for safe consumption, following standard guidelines [81, 82]. These values are presented in Table 1.

Since the spectrometer developed by Natthasak and Suchart [36] measured pesticide residue levels on chili using the reflectivity power density of incident light in [μW/cm^2], it was necessary to convert the MRL threshold values in Table 1 from [mg/L] into [μW/cm^2] This conversion was achieved using the exponential model in Eq. (11), providing the MRL threshold values in Table 2. The obtained result is compared with results from PLSR, line equation, and quadratic models.

***Table 1**: MRL of the four pesticides on the chili seeds in the unit of [mg/L].*

MRL [mg/L]			
Carbendazim ($i = 1$)	**Cypermethrin ($i = 2$)**	**Diazinon ($i = 3$)**	**Imidacloprid ($i = 4$)**
2	2	0.01	0.01

***Table 2**: MRL of the four pesticides on the chili in the unit of [$\mu W/cm^2$].*

Model	**MRL [$\mu W/cm^2$]**			
	Carbendazim ($i = 1$)	**Cypermethrin ($i = 2$)**	**Diazinon ($i = 3$)**	**Imidacloprid ($i = 4$)**
Line	δ_1^L	δ_2^L	δ_3^L	δ_4^L
Quadratic	δ_1^Q	δ_2^Q	δ_3^Q	δ_4^Q
PLSR	δ_1^P	δ_2^P	δ_3^P	δ_4^P
Propose	δ_1	δ_2	δ_3	δ_4

Each of the parameter δ_i as shown in Table 2 is the MRL threshold value in the unit of [μW/cm^2] for each type of the four pesticide residues: Carbendazim, Cypermethrin, Diazinon and Imidacloprid in cases of i=1,2,3 and 4, respectively. When substituting $n = 2$ [mg/L] into the exponential model developed in the relationship (11), both δ_1 and δ_2 values are equal to $y_i[2]$ in the unit of [μW/cm^2]; that is,

$$\delta_1 = \delta_2 = a_1^0(a_2^0)^2 + a_0^0 e^2 \tag{16}$$

Likewise, when substituting $n = 0.01$ [mg/L] into the developed model in the Eq. (11), both δ_3 and δ_4 values are also equal to $y_i[0.01]$ in the unit of [μW/cm^2], which are given by

$$\delta_3 = \delta_4 = a_0^0 e^0.01 + a_1^0(a_2^0)^0.01 \tag{17}$$

In addition, the threshold values obtained from the Line and Quadratic models are generated for each pesticide residues, as shown in the line two and the line three of Table 2. The threshold values obtained from the Line equation model in Eq. (1) are defined as follows:

$$\delta_1^L = \delta_2^L = a_0 + 2a_1^n \tag{18}$$

, and

$$\delta_3^L = \delta_4^L = a_0 + 0.01a_1^n \tag{19}$$

Similarly, the threshold values obtained from the Quadratic model in Eq. (2) are given by

$$\delta_1^Q = \delta_2^Q = a_0 + 4a_1 + 2a_2 \tag{20}$$

, and

$$\delta_3^Q = \delta_4^Q = a_0 + 10^{-4}a_1 + 0.01a_2 \tag{21}$$

For criteria values derived from the PLSR model in equation (3), the criteria values δ_1^P and δ_2^P are set equal to the MSPD value at a concentration of 2 mg/L. Meanwhile, the values δ_3^P and δ_4^P are approximated outside the range using the linear interpolation method [90]. The resulting criteria correspond to the MSPD value at a concentration of 0.01 mg/L.

The output MSPD ($y_i[n]$) is compared to the MRL [μW/cm^2]. $y_i[n]$ are classified as "Safe" if the $y_i[n] \leq \boldsymbol{MRL}$ [μW/cm^2] and "Unsafe" if it exceeds $\boldsymbol{MRL}$ [μW/cm^2].

Following the optimum parameter of the four models performed ten-times cross-validation with the 4:1 train/test data ratio to enhance model reliability and robustness, and after computing the MRL thresholds in [μW/cm²] for each pesticide using the proposed exponential model and the other models ($\delta_i, \delta_i^P, \delta_i^Q, \delta_i^L$), the models will be evaluated in terms of: prediction accuracy of the MRL values, and classification performance in determining the safety levels ("Safe" or "Unsafe") on the test dataset. The methods and evaluation metrics used for this performance assessment are described in the following section.

2.3 Model Performance and Evaluation

To evaluate the performance of the developed model in estimating the output element of the power density of the incident light on pesticide residues on chili seeds, two indicators; that is, the *R*-squared value (R^2) and the root mean square error (RMSE) were used in this research. Each of the two indicators is a crucial measure of how well the developed model fits the estimated values of the output power density sequence $\{y_i[n]\}$ for $i \in \{1, 2, 3, 4\}$ and $n \in \{1, 2, 3, \ldots, 10\}$. For a given input power density sequence $\{x_i[n]\}$ for $i \in \{1, 2, 3, 4\}$ and $n \in \{1, 2, 3, \ldots, 10\}$, the *R*-squared value is defined as

$$R^2 = 1 - \frac{\sum_{n=1}^{10} (x_i[n] - y_i[n])^2}{\sum_{n=1}^{10} (x_i[n] - \mu)^2} \tag{22}$$

The μ value is the average of the input MSPD sequence $\{x_i[n]\}$ for $i \in \{1, 2, 3, 4\}$, and the μ value is simplify specified by

$$\mu = \frac{1}{10} \sum_{n=1}^{10} x_i[n] \tag{23}$$

It is clear that the R-squared value provides the percentage of variation in the estimated values of the output MSPD sequence $\{y_i[n]\}$ described by the input MSPD sequence $\{x_i[n]\}$ at a given pesticide concentration [mg/L] for $n \in \{1, 2, 3, \ldots, 10\}$.

The R^2 value range is less than or equal to one. If the R^2 value is one, the variance in the error data is zero; that is the model perfectly generates the estimated data, while if the R^2 value is zero, it means that the model provides the estimated data using the mean to predict. In general, if the R^2 values are greater than 0.8, then the prediction model is considered to be acceptable, and if the R^2 values are greater than 0.9, then the model is indicated to be high accuracy [83–84].

Then, the other indicator in measuring the model performance in this research is the RMSE value. The RMSE value offers a magnitude measure of the prediction error in the same unit as the power density. For a given input MSPD sequence $\{x_i[n]\}$ for $i \in \{1, 2, 3, 4\}$ and $n \in \{1, 2, 3, \ldots, 10\}$, the RMSE is defined as

$$\text{RMSE} = \sqrt{\frac{1}{10} \sum_{n=1}^{10} (x_i[n] - y_i[n])^2} \tag{24}$$

The RMSE value range is greater than or equal to zero. If the RMSE value is zero, the deviation between the input and output MSPD is zero; that is, the model perfectly generates the output MSPD. Increased RMSE values reflect greater differences between input / output MSPD.

The model's performance in classifying output MSPD as "Safe" or "Unsafe" is evaluated using a test dataset of 160 samples, which includes 32 "Safe" cases and 128 "Unsafe" cases (a 1:4 ratio). Due to this class uneven distribution, both Accuracy and the Harmonic Mean of Recall and Specificity (HMRS) are used to ensure a comprehensive evaluation. This approach assesses not only the overall accuracy, but also the model's ability to correctly identify the underrepresented "Safe" class.

Accuracy is calculated as:

$$\text{Accuracy} = \frac{(TP + TN)}{(TP + TN + FP + FN)} \tag{25}$$

It is clear that TP and TN are the number of times that the developed model correctly predicts the "Safe" and "Unsafe" MSPD, respectively. FP is the number of the "Safe" MSPD sample that is wrongly predicted to be "Unsafe", but FN is the number of the "Unsafe" MSPD sample that is wrongly predicted to be "Safe", Although Accuracy is a good metric for evaluating the overall correctness of a model, but it may not clearly reflect the performance difference between "Safe" and "Unsafe" cases, Therefore, additional metrics are needed to assess accuracy in each specific case. In general, Recall is used to measure the model's ability to correctly identify "Safe" cases, while Specificity measures its ability to correctly identify "Unsafe" cases. In this research, both the Recall and the Specificity are simplified into a single metric by using the harmonic mean of the two values, which is called "HMRS" and can be expressed as follows:

$$\text{HMRS} = \frac{2}{\frac{1}{\frac{TP}{TP+FN}} + \frac{1}{\frac{TN}{TN+FP}}}$$

, or

$$\textbf{HMRS} = \frac{2 \times TP \times TN}{(TP \times (TN + FP) + TN \times (TP + FN)} \tag{26}$$

The HMRS value is a metric that evaluates the ability of the developed model to identify either a "Safe" case in terms of "Specificity" or an "Unsafe" case in terms of "Recall." It provides the performance to be evaluated even if there is a different proportion of the "Safe" and "Unsafe" cases; therefore, it is necessary to add the HMRS value to measure the accuracy of the different proportion of the two cases. The developed model will be highly efficient if and only if both the Accuracy and HMRS values are close to one. If the HMRS value remains low despite a very high Accuracy value, the developed model is still considered to be low in efficiency. Furthermore, the HMRS value cannot be calculated in the case of a situation where only one class occurs. However, such a case is difficult to occur since the test samples contain both classes in this research. The four previous metrics: R^2, RMSE, Accuracy and HMRS described in this section focus on selecting metrics based on the error distribution between the MSPD prediction data and the MSPD original data, which is used as the input for the developed model. This idea follows Sokolova et al. [85], and also focuses on selecting metrics to consider the impact of such errors following the idea of Koutsandreas et al. [86]. The next section will verify the effective results of testing the performance of the developed model in identifying "Safe" and "Unsafe" cases for 480 samples of pesticide residues on chili seeds.

3. RESULTS AND DISCUSSION

In this section, the performance and evaluation results of the developed model will be presented to determine the threshold value of each pesticide residue on chili, and the threshold value is then applied to test the accuracy of a group of pesticide residues on chili. The outline of this section consists of the results of the MSPD data collection obtained from the incident light on chili, the performance results of the developed model, and the accuracy results in determining the safety level of pesticide residues on chili seeds.

3.1 MSPD Data Collection Results

The results of spectral reflectance data collection for the four pesticide residues at concentrations ranging from 1-10 [mg/L] on chili samples, following the procedures outlined in Section 2.1, are shown in Fig. 2(a)–(d). Each graph displays the power density [μW/cm^2] of measured light at wavelengths from 410 nm to 910 nm for each type of pesticide residue, namely carbendazim, cypermethrin, diazinon, and imidacloprid.

From the power density of the diffuse reflectance spectra in Fig. 2, it is shown that the peak value of the power density occurs at the same wavelength position across all concentrations for each of the four pesticide residues. It is also found that the wavelengths at the positions of maximum power density are 460 nm, 535 nm, 900 nm, and 810 nm for carbendazim residues in Fig. 2(a), cypermethrin residues in Fig. 2(b), diazinon residues in Fig. 2(c), and imidacloprid residues in Fig. 2(d), respectively. These peak values of power density for the four given pesticide residues are the same as those found by Natthasak and Suchart [36]. Next, the peak values of the power density for each pesticide concentration were then generated as a data sequence; that is, the MSPD sequence $\{x_i[n]\}$ in the unit of [μW/cm²] with respect to pesticide concentration (n) in the unit of [mg/L] for $n \in \{1, 2, 3, \ldots, 10\}$, as shown in Fig. 3(a), Fig. 3(b), Fig. 3(c), and Fig. 3(d) for ($i = 1$) carbendazim residues, ($i = 2$) cypermethrin residues, ($i = 3$) diazinon residues and ($i = 4$) imidacloprid residues, respectively.

***Table 3**: A classification level of the 160 test samples.*

Classification levels	Number of test samples				
	($i = 1$)	($i = 2$)	($i = 3$)	($i = 4$)	Total
"Safe"	8	8	8	8	32
"Unsafe"	32	32	32	32	128

After preparing the training dataset as the input data sequence $\{x_i[n]\}$ for finding all optimum parameters of the developed model in the spectral data collection process, the next step is to verify the evaluation accuracy of the developed model to identify the test samples of pesticide residues on chili, whether they are safe or not. The test set consists of a total 160 samples, comprising 40 samples per pesticide. There are ten concentration levels for each of the four test pesticides, in which the concentration levels for carbendazim and cypermethrin are 1, 2, ..., 9 and 10 [mg/L], and those for diazinon and imidacloprid are 0.005, 0.01, 1, 2, ..., 7 and 8 mg/L. There are four samples for each of the ten concentration levels. The test data set of 160 samples is classified as either a "Safe" case or an "Unsafe" case for consumers, strictly following the MRL criteria. According to the classification process conducted in the main laboratory under ISO/IEC 17025:2005 and ISO/IEC 17025:2017 standards, it is verified that the "Safe" case for carbendazim and cypermethrin is less than or equal to 2 [mg/L], and for diazinon and imidacloprid, it is less than or equal to 0.01 [mg/L]. Finally, Table 3 shows a classification summary of the total 160 samples, identifying 32 samples as the "Safe" level and 128 samples as the "Unsafe" level. The ratio of the "Safe" level to the "Unsafe" level is 1:4. This means that 8 samples are classified as the "Safe" level and 32 samples as the "Unsafe" level for each of the four pesticides: carbendazim ($i = 1$), cypermethrin ($i = 2$), diazinon ($i = 3$) and imidacloprid ($i = 4$). The 160 test samples are used to evaluate their classification performance.

3.2 Results about the Proposed Model Efficiency

The MSPD sequence $\{x_i[n]\}$ with respective to a pesticide concentration (n) for $n \in \{1, 2, 3, \ldots, 10\}$ as an input sequence to the proposed model, the PLSR model, the quadratic model, and the line equation models to produce the predicted output MSPD sequence $\{y_i[n]\}$ as shown in Table 4. The optimum parameters in Table 5

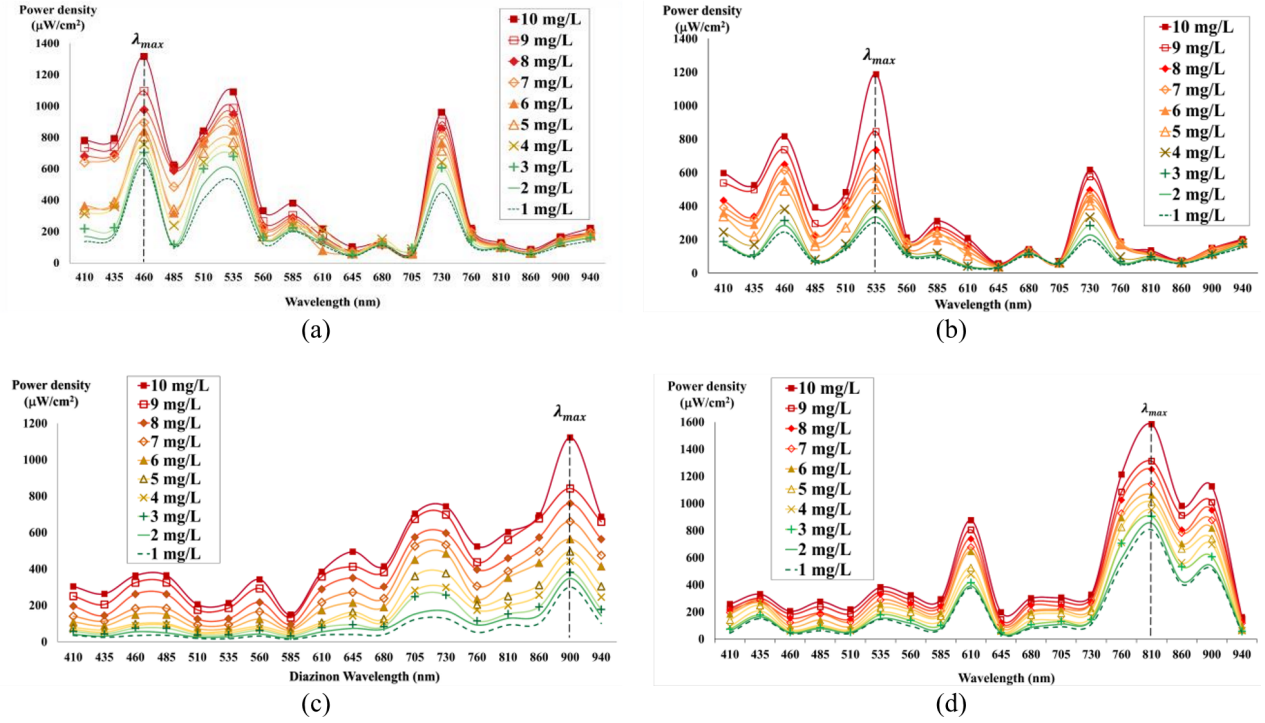

***Fig. 2**: Diffuse Reflectance Spectra of Four Pesticides at Various Concentrations: (a) Carbendazim (b) Cypermethrin (c) Diazinon (d) Imidacloprid.*

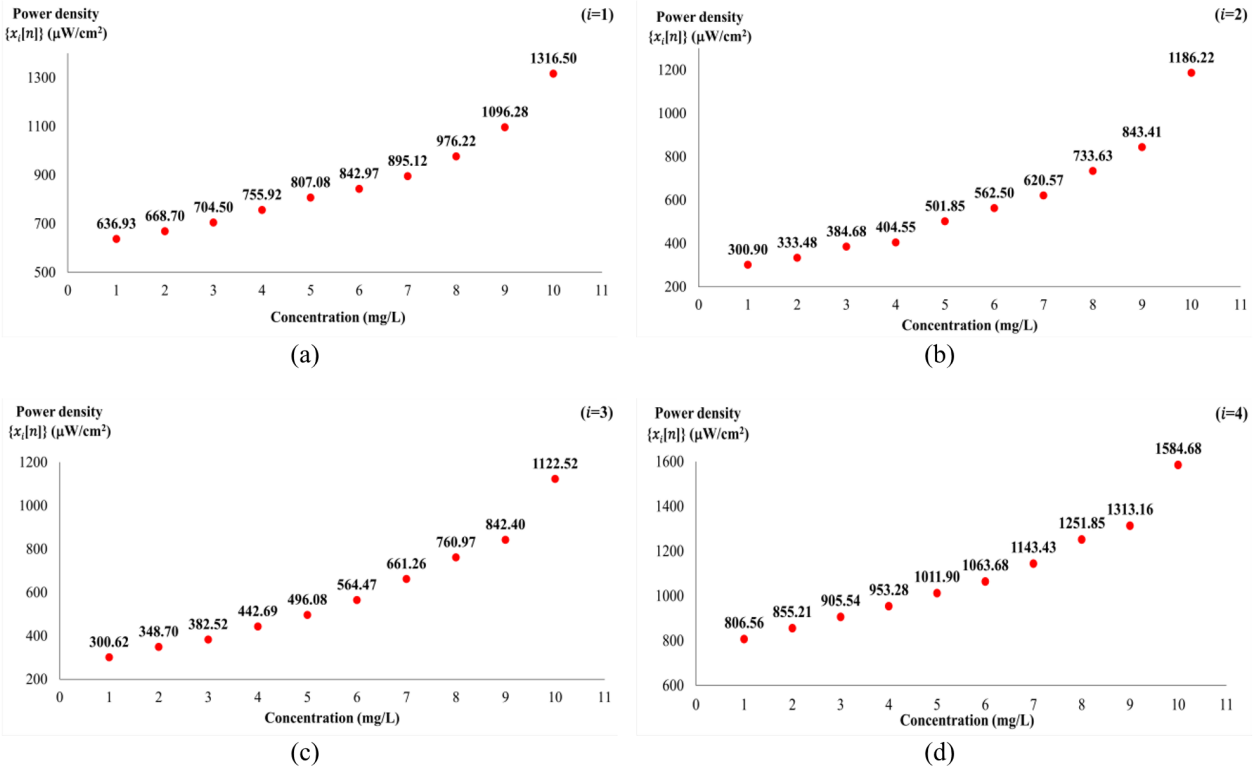

***Fig. 3**: MSPD [$\mu W/cm^2$] from Chili Spectra with Pesticide (a) Carbendazim, (b) Cypermethrin, (c) Diazinon, and (d) Imidacloprid.*

of the four models, calculated by using the least squares regression (LSR), are discussed in Section 2.

Fig. 4 shows a plot of the MSPD input data $x_i[n]$ in [μW/cm^2] and four MSPD output data $y_i[n]$ in [μW/cm^2]

***Table 4**: MSPD Values in [$\mu W/cm^2$] of Input $x_i[n]$ and Output $y_i[n]$ for Four Pesticides $i \in \{1,2,3,4\}$ at Ten Different Concentrations $n \in \{1,2,3,\ldots,10\}$ in [mg/L].*

Pesticide types	Items	MSPD values [μW/cm²]									
	Concentration n $[mg/L]$	1	2	3	4	5	6	7	8	9	10
Carbendazim	Input data $x_1[n]$	636.93	668.70	704.50	755.92	807.08	842.97	895.12	976.22	1096.28	1316.50
	Line output data $y_1[n]$	572.19	638.38	704.57	770.76	836.95	903.14	969.33	1035.52	1101.71	1167.90
	Quadratic output data $y_1[n]$	644.57	668.94	701.70	742.86	792.43	850.38	916.74	991.50	1074.65	1166.20
	PLSR	663.99	668.98	689.26	724.84	775.72	841.89	923.35	1020.11	1132.17	1259.52
	Proposed output data $y_1[n]$	634.90	671.65	710.62	752.09	796.65	845.67	902.60	976.68	1092.69	1317.74
Cypermethrin	Input data $x_2[n]$	300.90	333.48	384.68	404.55	501.85	562.50	620.57	733.63	843.41	1186.22
	Line output data $y_2[n]$	205.77	290.54	375.31	460.08	544.85	629.62	714.39	799.16	883.93	968.70
	Quadratic output data $y_2[n]$	350.82	369.98	407.38	463.02	536.90	629.02	739.38	867.98	1014.82	1179.90
	PLSR	334.06	333.26	353.86	395.86	459.25	544.05	650.24	777.83	926.82	1097.21
	Proposed output data $y_2[n]$	304.23	341.02	382.35	428.98	482.05	543.77	618.99	719.77	877.52	1176.07
Diazinon	Input data $x_3[n]$	300.62	348.7	382.52	442.69	496.08	564.47	661.26	760.97	842.4	1122.52
	Line output data $y_3[n]$	224.83	306.46	388.09	469.72	551.35	632.98	714.61	796.24	877.87	959.50
	Quadratic output data $y_3[n]$	305.20	340.16	384.6	438.40	501.7	574.5	656.7	748.4	849.5	960
	PLSR	326.01	340.25	371.33	419.25	484.03	565.65	664.12	779.43	911.60	1060.61
	Proposed output data $y_3[n]$	306.60	346.01	390.54	440.98	498.40	564.57	642.97	741.59	880.48	1112.23
Imidacloprid	Input data $x_1[n]$	806.56	855.21	905.54	953.28	1011.90	1063.68	1143.43	1251.85	1313.16	1584.68
	Line output data $y_4[n]$	746.34	822.48	898.62	974.76	1050.90	1127.04	1203.18	1279.32	1355.46	1431.60
	Quadratic output data $y_4[n]$	812.48	851.93	898.14	951.11	1010.85	1077.35	1150.62	1230.65	1317.44	1411.00
	PLSR	861.29	885.88	923.21	973.30	1036.14	1111.73	1200.07	1301.16	1415.00	1541.59
	Proposed output data $y_4[n]$	809.56	855.36	903.82	955.26	1010.26	1070.12	1138.14	1222.99	1347.94	1575.93

***Table 5**: Regression optimum parameters obtained from the proposed, PLSR, quadratic, and line equation models.*

Pesticide types	Model	Parameters		
		a_0	a_1	a_2
Carbendazim	Line	506.000	66.190	-
	Quadratic	628.600	11.770	4.199
	PLSR	674.290	-17.954	7.648
	Proposed	0.012	1.058	600.170
Cypermethrin	Line	121.000	84.770	-
	Quadratic	349.900	-8.200	9.120
	PLSR	356.260	-32.896	10.699
	Proposed	0.015	1.121	271.430
Diazinon	Line	143.200	81.630	-
	Quadratic	328.500	-11.010	8.420
	PLSR	279.700	20.780	4.730
	Proposed	0.009	1.128	271.690
Imidacloprid	Line	670.200	76.140	-
	Quadratic	779.800	29.300	3.382
	PLSR	849.460	5.458	6.376
	Proposed	0.011	1.056	766.240

***Table 6**: Efficiency of the four models for the four pesticides (R^2 and RMSE).*

Pesticide	Model	R^2	RMSE
Carbendazim	Line	0.898	64.013
	Quadratic	0.939	49.259
	PLSR	0.975	31.896
	Proposed	0.999	5.015
Cypermethrin	Line	0.944	90.813
	Quadratic	0.949	86.602
	PLSR	0.985	46.898
	Proposed	0.998	16.952
Diazinon	Line	0.965	69.254
	Quadratic	0.980	51.856
	PLSR	0.992	32.416
	Proposed	0.998	15.432
Imidacloprid	Line	0.959	63.474
	Quadratic	0.968	55.658
	PLSR	0.974	50.412
	Proposed	0.998	14.859

with respect to ten concentrations $n \in \{1,2,3,\ldots,10\}$ in [mg/L] for each of the four pesticides: carbendazim, cypermethrin, diazinon, and imidacloprid. The MSPD values obtained from the measured data by the developed method [36] and the estimated MSPD data generated by the four models for each of the ten concentrations are shown in Fig. 4. The proposed model provides the best estimation when compared to the estimations of the line equation, quadratic and PLSR models.

From Table 6, the proposed model can achieve the highest R-square score and the lowest RMSE values when compared to the three models, especially the PLSR method corresponding with previous studies by Aira et al. [26], Dinesha et al. [27], and Li et al. [91] for predicting glyphosate, coragen, toxins in cauliflower, respectively.

Then, the threshold value in [μW/cm^2] for each of the four pesticides, calculated from the estimated data of the four model, as shown in Fig. 5, and determined in the fourth line in Table 7 to classify the safety level in terms of the MSPD value according to the MRL standard criteria [81,82]. It is found that the proposed model's MRL threshold values in [μW/cm²] is 671.65, 341.02, 277.03 and 766.67 for carbendazim, cypermethrin, diazinon, and imidacloprid, respectively. The remaining threshold values from the line equation, quadratic and

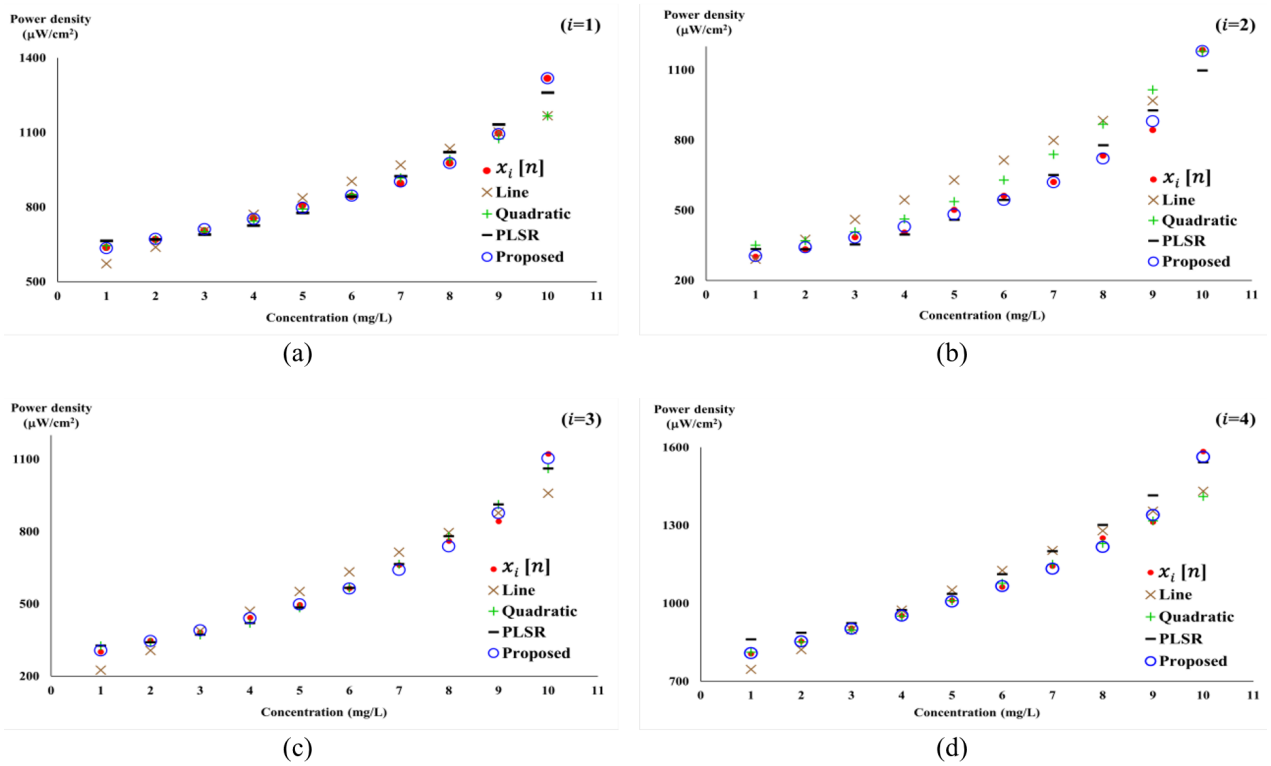

***Fig. 4**: A plot of the MSPD input data $x_i[n]$ in $[\mu W/cm^2]$ and four MSPD output data $y_i[n]$ in $[\mu W/cm^2]$ with respect to ten different concentrations $n \in \{1, 2, 3, \ldots, 10\}$ in [mg/L] for each of four pesticide residues: (a) Carbendazim, (b) Cypermethrin, (c) Diazinon, and (d) Imidacloprid.*

***Table 7**: MRL Threshold of four Pesticides on the Chili.*

Model	MRL $[\mu W/cm^2]$			
	Carbendazim	Cypermethrin	Diazinon	imidacloprid
Line	638.38	290.54	144.02	670.96
Quadratic	668.94	369.98	328.39	780.09
PLSR	668.97	333.26	279.91	849.51
Proposed	671.65	341.20	272.02	766.67

PLSR models are shown in the first, second and third lines, respectively.

These threshold values are used to classify the safety level. If the MSPD is less than the given threshold value, this means “Safe”, and if not, this means “Unsafe”.

3.3 Proposed Model Evaluation Results

All threshold values in Table 7 are used for 160 test samples of the MSPD output data obtained from the line equation, quadratic, PLSR and proposed model to identify the safety level of each type of the four pesticides. In the evaluation of the model performance, Accuracy and HMRS indicators are applied and calculated from Eq. (23) and Eq. (24), respectively. Evaluation results in Table 8 clearly show the proposed model demonstrates superior predictive performance in both metrics.

Classification test results using the MRL-based threshold $[\mu W/cm^2]$ clearly demonstrate that the Proposed model can perfectly classify both ”Safe” and ”Unsafe” samples across all four pesticide types: carbendazim, cypermethrin, diazinon, and imidacloprid. It achieves Accuracy and HMRS values of 1.000 throughout all

***Table 8**: Evaluation of four models for four pesticides (Accuracy and HMRS).*

Pesticide	Model	Accuracy	HMRS
Carbendazim	Line	0.850	0.400
	Quadratic	0.975	0.933
	PLSR	0.975	0.933
	Proposed	1.000	1.000
Cypermethrin	Line	0.825	0.222
	Quadratic	0.975	0.984
	PLSR	0.950	0.857
	Proposed	1.000	1.000
Diazinon	Line	0.800	0.000
	Quadratic	0.900	0.933
	PLSR	1.000	1.000
	Proposed	1.000	1.000
Imidacloprid	Line	0.800	0.000
	Quadratic	0.975	0.984
	PLSR	0.900	0.933
	Proposed	1.000	1.000

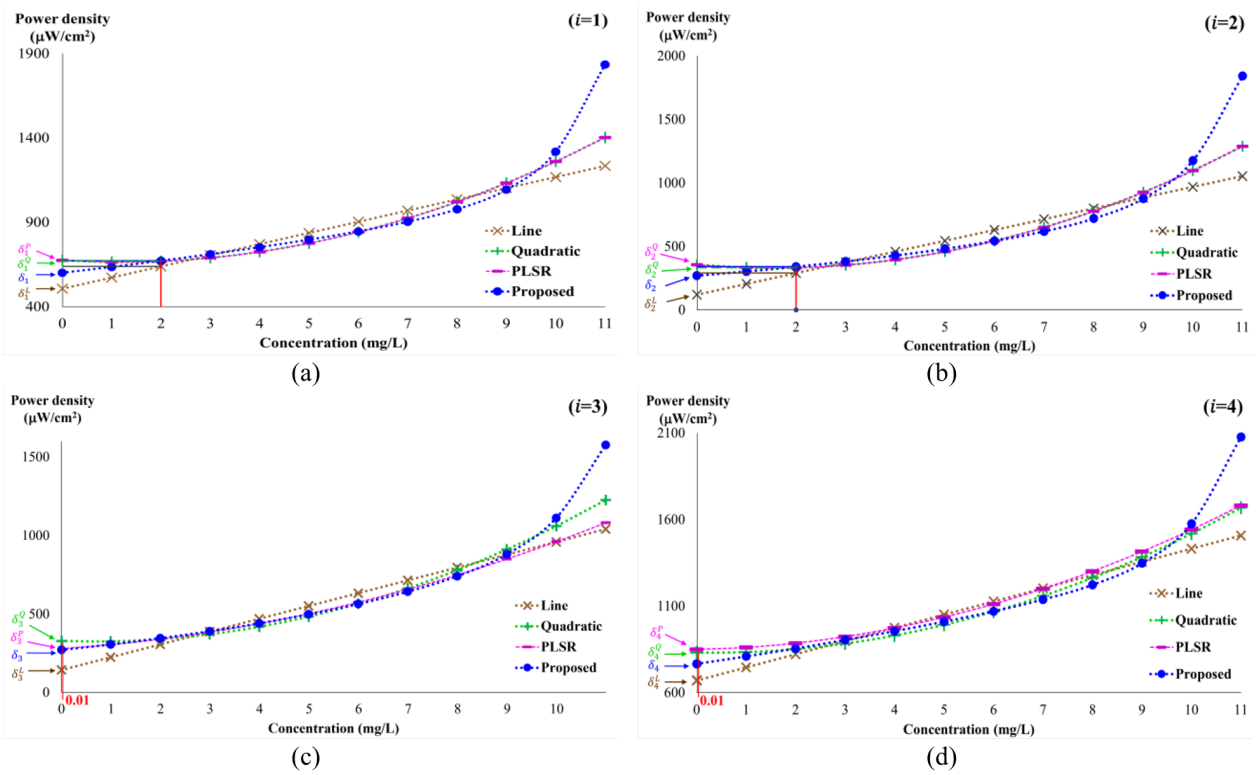

***Fig. 5**: The Output MSPD ($y_i[n]$) of four model and MRL [$\mu W/cm^2$] Based Safety Threshold Determination for Four Pesticides: (a) Carbendazim, (b) Cypermethrin, (c) Diazinon, and (d) Imidacloprid.*

testing. The proposed model outperforms the PLSR model, which has Accuracy values ranging from 0.900 to 1.000 and HMRS values between 0.875 and 1.000. The Proposed model shows a higher Accuracy of 0–10% and a higher HMRS of 0–12.5%. This difference is particularly notable in terms of HMRS values, which reflect a more balanced classification ability between "Safe" and "Unsafe" classes. Although the quadratic and line equation models provide Accuracy in the range from 0.800 to 0.975 and HMRS in the range from 0.000 to 0.984, they still cannot match the perfect classification performance of the Proposed model. This demonstrates the excellent ability of our new model to separate sample groups.

The main advantages of the proposed model requiring only three parameters are its simplicity and high performance for pesticide detection without requiring complex structures that consume high computing power and memory as machine learning algorithms (SVM/SVR, CNN) studied by Chang et al. [92], Orăsan et al. [93], and Rego et al. [94], which make them unsuitable for resource-limited embedded systems.

4. CONCLUSION

The proposed model provides an efficient and practical approach for determining the safety level of pesticide residues on fruits and vegetables through the estimation of optimal MSPD threshold values. This model, compatible with the portable spectrometer developed by Natthasak and Suchart [36], accurately predicts the MSPD values ($\mu W/cm^2$) of spectral signals resulting from incident light reflected from chili contaminated with four types of pesticides: carbendazim, cypermethrin, diazinon, and imidacloprid. It effectively models MSPD values across a concentration range of 1–10 mg/L for each pesticide. When compared to PLSR, quadratic, and linear models, the proposed model consistently achieves the highest R^2 and the lowest RMSE, demonstrating superior regression performance. Notably, the model achieves perfect classification accuracy and HMRS values of 1.000 for all pesticides and all cases, surpassing the performance of the baseline models, particularly under the MRL-based safety classification.

Beyond its predictive accuracy, the proposed model offers structural simplicity and computational efficiency. It requires the estimation of only three parameters per pesticide and uses a single MSPD variable as input, whereas PLSR relies on multiple latent variables derived from analyzing reflectance data across a wide wavelength spectrum. This simplicity reduces both model complexity and computational cost, making it highly suitable for real-time, portable, or embedded detection systems. Therefore, the proposed model not only ensures accurate prediction and robust safety classification but also offers practical advantages in terms of implementation, calibration, and processing speed.

ACKNOWLEDGEMENT

This work was supported by the Office of Agricultural Research and Development (Public Organization) and the Social Innovation Works Development Project, Social Innovation Driving Unit (SID) for the Lower Northern Region, National Innovation Agency Thailand (NIA), Ministry of Higher Education, Science, Research and Innovation.

REFERENCES

[1] Food and Agriculture Organization of the United Nations (FAO), Pesticides use and trade – 1990–2022, *FAOSTAT Analytical Briefs*, No. 89, Rome, 2024.

[2] World Health Organization (WHO), Compendium of WHO and other UN guidance on health and environment, 2022 update. *Geneva: World Health Organization*, 2022.

[3] FAO & WHO, *Report 2021 - Pesticide residues in food - Joint FAO/WHO Meeting on Pesticide Residues*. Rome. 2022.

[4] H. Pang et al., "Portable organophosphorus pesticide detection device based on controllable microfluidic and luminol composite nanofibers," *Journal of Food Engineering*, vol. 364, p. 111810, Oct. 2023.

[5] A. Yazici, G. Y. Tiryaki, and H. Ayvaz, "Determination of pesticide residual levels in strawberry (Fragaria) by near-infrared spectroscopy," *Journal of the Science of Food and Agriculture*, vol. 100, no. 5, pp. 1980–1989, Dec. 2019.

[6] A. Szarka and S. Hrouzková, "FAST DLLME-GC-MS method for determination of pesticides in carmelite drops and evaluation of matrix effects in related medicinal products," *Foods*, vol. 13, no. 11, p. 1745, Jun. 2024.

[7] S. T. Narenderan, S. N. Meyyanathan, and B. Babu, "Review of pesticide residue analysis in fruits and vegetables. Pre-treatment, extraction and detection techniques," *Food Research International*, vol. 133, p. 109141, Mar. 2020.

[8] L. Luo et al., "Detection and risk assessments of multi-pesticides in 1771 cultivated herbal medicines by LC/MS-MS and GC/MS-MS," *Chemosphere*, vol. 262, p. 127477, Aug. 2020.

[9] G. Kowalska, U. Pankiewicz, and R. Kowalski, "Estimation of Pesticide Residues in Selected Products of Plant Origin from Poland with the Use of the HPLC-MS/MS Technique," *Agriculture*, vol. 10, no. 6, p. 192, Jun. 2020.

[10] S. Shrestha, B. Lamichhane, and N. Chaudhary, "Method validation and measurement uncertainty Estimation for determination of multiclass pesticide residues in tomato by Liquid Chromatography-Tandem Mass Spectrometry (LC-MS/MS)," *International Journal of Analytical Chemistry*, vol. 2024, pp. 1–10, Jan. 2024.

[11] T. S. Nteping, M. N. Alakeh, N. E. B. Tamungang, and T. M. Awah, "Analysis of pesticide residues in some market garden crops in Santa, north West Cameroon," *Journal of Environmental Protection*, vol. 13, no. 05, pp. 331–343, Jan. 2022.

[12] S. F. Hosseini, H. Nassehinia, H. Nazari, Y. D. Shahamat, Z. Ghoraba, and K. Moeinian, "Determination of diazinon concentration by Gas Chromatography - Mass Spectrometry in underground drinking water resources located near the rice fields, before and after the pesticide spraying," *Microchemical Journal*, vol. 170, p. 106600, Jul. 2021.

[13] A. S. Tsagkaris, J. Pulkrabova, and J. Hajslova, "Optical Screening Methods for pesticide residue detection in food matrices: Advances and emerging analytical trends," *Foods*, vol. 10, no. 1, p. 88, Jan. 2021.

[14] S. N. Zainurin, W. Z. W. Ismail, W. A. N. W. Azlan, K. N. Z. Ariffin, and W. M. W. A. Kamil, "Developing a portable spectrometer to detect chemical contaminants in irrigation water," *Agriculture*, vol. 13, no. 6, p. 1202, Jun. 2023.

[15] A. S. Nazarloo, V. R. Sharabiani, Y. A. Gilandeh, E. Taghinezhad, M. Szymanek, and M. Sprawka, "Feasibility of using VIS/NIR spectroscopy and multivariate analysis for pesticide residue detection in tomatoes," *Processes*, vol. 9, no. 2, p. 196, Jan. 2021.

[16] S. Heydarov, M. Aydin, C. Faydaci, S. Tuna, and S. Ozturk, "Low-cost VIS/NIR range hand-held and portable photospectrometer and evaluation of machine learning algorithms for classification performance," *Engineering Science and Technology an International Journal*, vol. 37, p. 101302, Nov. 2022.

[17] A. S. Nazarloo, V. R. Sharabiani, Y. A. Gilandeh, E. Taghinezhad, and M. Szymanek, "Evaluation of different models for Non-Destructive Detection of tomato pesticide residues based on Near-Infrared Spectroscopy," *Sensors*, vol. 21, no. 9, p. 3032, Apr. 2021.

[18] R. Li, H. Wang, B. Shen, and X. Yao, "Study on Dissipation Law of pesticides in Cauliflower based on Hyperspectral Image Technique," *Agriculture*, vol. 13, no. 12, p. 2254, Dec. 2023.

[19] F. S. Rodriguez et al., "NIR spectroscopy detects Chlorpyrifos-Methyl pesticide residue in rough, brown, and milled rice," *Applied Engineering in Agriculture*, vol. 36, no. 6, pp. 983–993, Jan. 2020.

[20] L. Sun, X. Cui, X. Fan, X. Suo, B. Fan, and X. Zhang, "Automatic detection of pesticide residues on the surface of lettuce leaves using images of feature wavelengths spectrum," *Frontiers in Plant Science*, vol. 13, Jan. 2023.

[21] L. Salguero-Chaparro, A. J. Gaitán-Jurado, V. Ortiz-Somovilla, and F. Peña-Rodríguez, "Feasibility of using NIR spectroscopy to detect herbicide

residues in intact olives," *Food Control*, vol. 30, no. 2, pp. 504–509, Aug. 2012.

[22] K. B. Beć, J. Grabska, and C. W. Huck, "Miniaturized NIR spectroscopy in food Analysis and Quality Control: promises, challenges, and perspectives," *Foods*, vol. 11, no. 10, p. 1465, May 2022.

[23] A. Ducanchez, S. Moinard, G. Brunel, R. Bendoula, D. Héran, and B. Tisseyre, "The AS7265X chipset as an alternative Low-Cost multispectral sensor for agriculture applications based on NDVI," in *Sense the Real Change: Proceedings of the 20th International Conference on Near Infrared Spectroscopy, 2022*, pp. 201–206.

[24] L. Duncan et al., "Weed Warden: A low-cost weed detection device implemented with spectral triad sensor for agricultural applications," *HardwareX*, vol. 11, p. e00303, Apr. 2022.

[25] M. Noguera, B. Millan, and J. M. Andújar, "New, Low-Cost, Hand-Held Multispectral Device for In-Field Fruit-Ripening Assessment," *Agriculture*, vol. 13, no. 1, p. 4, Dec. 2022.

[26] J. Aira, T. Olivares, and F. M. Delicado, "SpectroGLY: a Low-Cost IoT-Based ecosystem for the detection of glyphosate residues in waters," *IEEE Transactions on Instrumentation and Measurement*, vol. 71, pp. 1–10, Jan. 2022.

[27] B. Dinesha, S. Hiregoudar, V. Kumar, U. Nidoni, and A. Shreenivas, "Modelling and simulation of eco-friendly nano-composite based dispenser for controlled release of agrochemicals," *International Journal of Chemical Studies*, vol. 8, no. 1, pp. 2508–2513, Jan. 2020.

[28] E. Zohar, H. Cohen, N. Goldshlager, S. Barel, and Y. Anker, "Detection of the amitraz pesticide in bee wax by hyperspectral imaging," *Journal of Food Measurement & Characterization*, vol. 18, no. 4, pp. 3008–3017, Mar. 2024.

[29] Z. Zhang, "Multivariable fractional polynomial method for regression model," *Annals of Translational Medicine*, vol. 4, no. 9, p. 174, May 2016.

[30] T. A. Ishola, O. T. Olabisi, and A. K. Kehinde, "Parameter estimation of fractional trigonometric polynomial regression model," *Journal of University of Babylon for Pure and Applied Sciences*, vol. 27, no. 1, pp. 519–526, May 2019.

[31] E. Ostertagová, "Modelling using Polynomial Regression," *Procedia Engineering*, vol. 48, pp. 500–506, Jan. 2012.

[32] Elshewey, Ahmed M. "An Optimized Ensemble Model for Inflation Prediction in Egypt." *American Journal of Business and Operations Research*, vol.10, no.2, pp. 61, 2023.

[33] N. Zahedi, A. A. Kamil, N. Jelita, H. Amin, A. Marwan, and S. Suparni, "Some applications of cubic equations in engineering," *Mathematical Modelling and Engineering Problems*, vol. 9, no. 1, pp. 129–135, Feb. 2022.

[34] J. J. Locascio and A. Atri, "An overview of longitudinal data analysis methods for neurological research," *Dementia and Geriatric Cognitive Disorders Extra*, vol. 1, no. 1, pp. 330–357, Oct. 2011.

[35] Y. Zhang et al., "Comparison and analysis of several quantitative identification models of pesticide residues based on quick detection paperboard," *Processes*, vol. 11, no. 6, p. 1854, Jun. 2023.

[36] N. Yaemsuk and S. Yammen, "Development of a portable NIR spectrometer for detecting pesticide residues," *Asian Health, Science and Technology Reports*, vol. 32, no. 1, pp. 32–48, Feb. 2024.

[37] International Organization for Standardization and International Electrotechnical Commission, *ISO/IEC 17025:2005 – General requirements for the competence of testing and calibration laboratories, 2nd ed.*, Geneva, Switzerland, 2005.

[38] International Organization for Standardization and International Electrotechnical Commission, *ISO/IEC 17025:2017 – General requirements for the competence of testing and calibration laboratories, 3rd ed.*, Geneva, Switzerland, Nov. 2017.

[39] T. A. Reddy and G. P. Henze, "Linear regression analysis using least squares," in *Springer eBooks*, 2023, pp. 169–221.

[40] P. Ding, "Linear Model and Extensions," *arXiv preprint arXiv:2401.00649*, Jan. 2024.

[41] V. Cecchi, M. Knudson, K. Miu, and C. Nwankpa, "A non-uniformly distributed parameter transmission line model," *2021 North American Power Symposium (NAPS)*, pp. 1–6, Sep. 2012.

[42] X. Gu and W. Zhang, "Application of the O-line model to martensite crystallography," *Science China Technological Sciences*, vol. 55, no. 2, pp. 464–469, Dec. 2011.

[43] I. M. Barbosa, B. N. Sismanoglu, and P. I. P. Oliveira, "FIRST DEGREE POLYNOMIAL FITTING FOR FORCES AND MOMENTS ON THE AERODYNAMIC TEST MODEL," Periódico Tchê Química, vol. 14, no. 27, pp. 97–104, Jan. 2017.

[44] S. Patil and S. Patil, "Linear with polynomial regression: Overview," *International Journal of Applied Research*, vol. 7, no. 8, pp. 273–275, Aug. 2021.

[45] B. Ghermoul, "Planar polynomial differential systems of degree one: Full characterization of its first integrals," *Research Square*, Sep. 2023.

[46] L.-J. Kao, T.-Y. Chen, and K.-C. Chang, "Efficient Mixture Design Fitting Quadratic Surface with Quantile Responses Using First-degree Polynomial," *Communications in Statistics - Simulation and Computation*, vol. 45, no. 4, pp. 1365–1380, May 2014.

[47] C. Starbuck, "Linear regression," in *Springer eBooks*, 2023, pp. 181–206.

[48] C. Wang, L. Zhu, and B. Jiang, "Penalized Interaction Estimation for Ultrahigh Dimensional Quadratic Regression," *Statistica Sinica*, Jan. 2021.

[49] M.-S. Moon, "Comparison of powers in goodness

of fit test of quadratic measurement error model," *Communications for Statistical Applications and Methods*, vol. 9, no. 1, pp. 229–240, Apr. 2002.

[50] C. Luo, H. Ding, and L. Zhu, "Two-Sided Quadratic Model for Workpiece Fixturing Analysis," *Journal of Manufacturing Science and Engineering*, vol. 133, no. 3, Jun. 2011.

[51] Z. Ren and Z. C. Hao, "Application of moving windows autoregressive quadratic model in runoff forecast," *International Conference on Industrial Mechatronics and Automation*, May 2009.

[52] J. Wood, "A quadratic model of consciousness," *Technoetic Arts*, vol. 13, no. 3, pp. 229–238, Dec. 2015.

[53] B. Wen et al., "A quadratic regression model to quantify plantation soil factors that affect tea quality," *Agriculture*, vol. 11, no. 12, p. 1225, Dec. 2021.

[54] S. M. Eldeeb and A. S. Fahmy, "Error analysis of fundus image registration using quadratic model transfformation," *2014 Cairo International Biomedical Engineering Conference (CIBEC)*, Giza, Egypt, 2014, pp. 137-140.

[55] Z. Sinuany-Stern, "Quadratic model for allocating operational budget in public and nonprofit organizations," *Annals of Operations Research*, vol. 221, no. 1, pp. 357–376, Jun. 2014.

[56] S. O. Woo et al., "Protein Detection using Quadratic Fit Analysis Near Dirac Point of Graphene Field Effect Biosensors.," *ACS applied electronic materials*, vol. 2, no. 4, pp. 913–919, Mar. 2020.

[57] I. Oloyede, "Bayesian Generalized Least Squares with Autocorrelated Error," *Deleted Journal*, vol. 4, no. 2, pp. 78–90, Oct. 2022.

[58] K. Thompson, "The sum of four squares over real quadratic number fields," *International Journal of Number Theory*, vol. 20, no. 01, pp. 47–72, Oct. 2023.

[59] L. Zhao, "The sum of divisors of a quadratic form," *Acta Arithmetica*, vol. 163, no. 2, pp. 161–177, Jan. 2014.

[60] S. Daniel, "On the sum of a square and a square of a prime," *Mathematical Proceedings of the Cambridge Philosophical Society*, vol. 131, no. 01, Jul. 2001.

[61] G. K. Smyth, "Nonlinear Regression-Extensions," Sep. 2014.

[62] E. Ostertagová, "Modelling using Polynomial Regression," *Procedia Engineering*, vol. 48, pp. 500–506, Jan. 2012.

[63] E. Matthew and O. Adeyinka, "Application of hierarchical polynomial regression models to predict transmission of COVID-19 at global level," *International Journal of Clinical Biostatistics and Biometrics*, vol. 6, no. 1, Jun. 2020.

[64] H. Zwart, "Linearization and exponential stability," *arXiv (Cornell University)*, Jan. 2014.

[65] B. Trivellato, "Sub-exponentiality in statistical exponential models," *Journal of Theoretical Probability*, vol. 37, no. 3, pp. 2076–2096, Aug. 2023.

[66] C. Pan, M. Pinto, and Y. Xia, "Exponential trichotomy and global linearization of non-autonomous differential equations," *arXiv (Cornell University)*, Jan. 2023.

[67] K. Saini, M. L. Dewal, and M. Rohit, "Spatial enhancement and modified log transformation for Echocardiographic images," *International Journal of Biomedical Engineering and Technology*, vol. 7, no. 4, p. 327, Jan. 2011.

[68] Guo Gang, Wang Shu-xun, Zhao Xiao-hui and Sun Xiao-ying, "Double exponential model of ultrasonic signals," *2008 9th International Conference on Signal Processing*, Beijing, 2008, pp. 2575-2578.

[69] O. Chevallier, N. Zhou, J.-P. Cercueil, J. He, R. Loffroy, and Y. X. J. Wáng, "Comparison of tri-exponential decay vs. bi-exponential decay and full fitting vs. segmented fitting for modeling liver intravoxel incoherent motion diffusion MRI," *bioRxiv (Cold Spring Harbor Laboratory)*, Sep. 2018.

[70] J. A. Ramos, "Exponential data fitting applied to environmental data," *2004 43rd IEEE Conference on Decision and Control (CDC) (IEEE Cat. No.04CH37601)*, vol. 10, pp. 4169-4174 Vol.4, Jan. 2004.

[71] O. Chevallier, N. Zhou, J. Cercueil, J. He, R. Loffroy, and Y. X. J. Wáng, "Comparison of tri-exponential decay versus bi-exponential decay and full fitting versus segmented fitting for modeling liver intravoxel incoherent motion diffusion MRI," *NMR in Biomedicine*, vol. 32, no. 11, Jul. 2019.

[72] E. Ostertagová, P. Frankovský and O. Ostertag, "Application of polynomial regression models for prediction of stress state in structural elements," *Global Journal of Pure and Applied Mathematics*, vol. 12, no. 4, pp. 3187–3199, Nov. 2016.

[73] E. Ostertagová, "Modelling using Polynomial Regression," *Procedia Engineering*, vol. 48, pp. 500–506, Jan. 2012.

[74] L. Grochova and L. StřElec, "Performance of the OLS estimator in presence of autocorrelation," *AIP Conference Proceedings*, pp. 1851–1854, Jan. 2013.

[75] S. Basiri, E. Ollila, G. Draskovic, and F. Pascal, "Fusing Eigenvalues," *ICASSP 2022 - 2022 IEEE International Conference on Acoustics, Speech and Signal Processing (ICASSP)*, pp. 4968–4972, Apr. 2019.

[76] W. Tang and J. Guo, "Eigenvalues and eigenfunctions of One-Dimensional fractal laplacians," *Journal of Nonlinear Mathematical Physics*, vol. 30, no. 3, pp. 996–1010, Apr. 2023.

[77] F. Ries, T. De Marco, and R. Guerrieri, "Triangular Matrix Inversion on Heterogeneous Multicore Systems," *IEEE Transactions on Parallel and Distributed Systems*, vol. 23, no. 1, pp. 177–184, Jan. 2012.

[78] Y. Choi, "New form of block matrix inversion," *IEEE/ASME International Conference on Advanced Intelligent Mechatronics*, pp. 1952–1957, Jul. 2009.

[79] K. Aliyeva, "Z-Matrix Consistency," in *Advances in*

intelligent systems and computing, 2019, pp. 841–845.

[80] R. Dwivedi and R. Sanjhira, "On the matrix function ${}_pR_q(A, B; z)$ and its fractional calculus properties," *arXiv (Cornell University)*, Jan. 2022.

[81] Government of Thailand, Thai Agricultural Standard (TAS 9002–2016): Pesticide Residues – Maximum Residue Limits [in Thai], The Royal Gazette, vol. 133, no. 288 D, Dec. 13, 2016.

[82] Codex Alimentarius Commission, "Pesticides," *FAO/WHO Codex Alimentarius*, 2025.

[83] H. Piepho, "An adjusted coefficient of determination (R2) for generalized linear mixed models in one go.," *Biometrical Journal*, vol. 65, no. 7, May 2023.

[84] J. Gao, "R-Squared (R2) – How much variation is explained?," *Research Methods in Medicine & Health Sciences*, vol. 5, no. 4, pp. 104–109, Dec. 2023.

[85] M. Sokolova and G. Lapalme, "A systematic analysis of performance measures for classification tasks," *Information Processing & Management*, vol. 45, no. 4, pp. 427–437, May 2009.

[86] D. Koutsandreas, E. Spiliotis, F. Petropoulos, and V. Assimakopoulos, "On the selection of forecasting accuracy measures," *Journal of the Operational Research Society*, vol. 73, no. 5, pp. 937–954, Apr. 2021.

[87] M. Lazorec, "PARTIAL LEAST SQUARES REGRESSION (PLSR) APPLIED FOR ASSESSING THE ECONOMIC RESILIENCE IN EU COUNTRIES," *Journal of Public Administration Finance and Law*, no. 28, pp. 180–199, Jan. 2023.

[88] J. Y.-L. Chan et al., "Mitigating the multicollinearity Problem and its machine Learning Approach: A review," *Mathematics*, vol. 10, no. 8, p. 1283, Apr. 2022.

[89] N. Zhang, K. Canini, S. Silva, and M. Gupta, "Fast linear interpolation," *ACM Journal on Emerging Technologies in Computing Systems*, vol. 17, no. 2, pp. 1–15, Apr. 2021.

[90] A. Pownuk and V. Kreinovich, "Why linear interpolation?," *Matematičeskie Struktury I Modelirovanie*, no. 3, pp. 43–49, Jan. 2017.

[91] M. Li, L. Lu, and X. Zhang, "Qualitative determination of pesticide residues in purple cabbage based on near infrared spectroscopy," *Journal of Physics Conference Series*, vol. 1884, no. 1, p. 012015, Apr. 2021.

[92] J. Chang, M. Kang, and D. Park, "Low-Power On-Chip implementation of enhanced SVM algorithm for sensors Fusion-Based activity classification in lightweighted edge devices," *Electronics*, vol. 11, no. 1, p. 139, Jan. 2022.

[93] I. L. Orășan, C. Seiculescu, and C. D. Căleanu, "A brief review of deep neural network implementations for ARM Cortex-M Processor," *Electronics*, vol. 11, no. 16, p. 2545, Aug. 2022.

[94] G. R. Fernández et al., "Portable IoT NIR Spectrometer for Detecting Undesirable Substances in Forages of Dairy Farms," *2019 International Conference on Sensing and Instrumentation in IoT Era (ISSI)*, Lisbon, Portugal, 2019, pp. 1-6.

[95] H. Wang, H. Xiang, T. Xiong, J. Feng, J. Zhang, and X. Li, "A straightforward approach utilizing an exponential model to compensate for turbidity in chemical oxygen demand measurements using UV-vis spectrometry," *Frontiers in Microbiology*, vol. 14, Jul. 2023.

[96] Y. Hu, R. Sandt, and R. Spatschek, "Practical feature filter strategy to machine learning for small datasets in chemistry," *Scientific Reports*, vol. 14, no. 1, Sep. 2024.

Natthasak Yaemsuk received the B.Eng degress in telecommunication and electrical engineering from Mahanakorn University of Technology, Thailand and M.Sc. degrees in computer science from Naresuan University, Thailand in 1998 and 2003, respectively. He works in Phitsanulok provincial agriculture and cooperatives office. His research interests include agricultural area database system and database system for safe saricultural products.

Suchart Yammen received the B.Eng degrees in electrical engineering from Chiang Mai University, Thailand and M.Sc. degrees and Ph.D. in electrical engineering from Vanderbilt University, USA in 1988, 1998, and 201, respectively. His research interests are Development of a product to detect residual pesticides in vegetables using near-infrared spectroscopy techniques to create safety for communities.